STM JOURNALS

Journal of
Aerospace Engineering & Technology

ISSN: 2231-038X (Online)
ISSN: 2348-7887 (Print)
Volume 15, Issue 3, 2025
September–December
DOI (Journal): 10.37591/JoAET

https://journals.stmjournals.com/joaet

Research JoAET

The Decision of the Maximum Synchronous Torque During the Solar Array Deployment Using the Closed Cable Loop

Hyon-Mu Jo, Song-Hyok Kim, Ji-Hyon Kim, Ju-Song Thak, Yong-Gil Han*

Abstract

It was a long time since mankind explored and studied the universe, but the early-age power sources have not changed a lot over that period. Solar panels have been used long ago and are still in use today. However, their efficiency has improved considerably. Large and complicated solar arrays are now used instead of simply attaching the panels directly on the face of the satellite. A solar array is essential for a spacecraft to carry out its mission successfully and the first task for the spacecraft in space is the deployment of the solar array. Since there is not much space in the nose cone of the launch vehicle, a stowed position of the solar panels is required. Also, during launch and ascent, the launch loads can be transmitted to the satellite structure in a better way, because of the stiffness of the solar array in the stowed configuration and its ability to take up high natural frequencies. A solar array is attached to the satellite by means of a yoke. The purpose of the yoke is to keep the array out of the satellite's own shadow, and several solar panels are connected by a rotating hinge here. In general, these solar arrays are deployed synchronously by a synchronous mechanism. The synchronization system controls the relative movement of the yoke and the panels with respect to the sidewall of the satellite. Hereby interference of the solar array with the satellite is prevented. The closed cable loop (CCL) is a typical synchronous mechanism for the solar array deployment. The closed cable loop device is known as a suitable instrument for deploying solar array configurations and arrays. This study provides a multi-DOF dynamic model of a solar array with n panels using the CCL. A formula to calculate the synchronous torque for the ideal synchronization is derived from the dynamic model, and its characteristics are analyzed. And then, the decision method of the maximum synchronous torque is provided. The calculation results indicate that the method is accurate enough and can be used to determine the CCL design parameters.

Keywords: Solar array, deployment, multi-DOF dynamic model, synchronous torque, linkage

INTRODUCTION

The primary electrical power of a spacecraft is obtained from a solar array and the first task of spacecraft in space is the deployment of the solar arrays. The typical solar array used in satellites consists of a yoke and several panels. The multiple panel solar arrays are usually folded during the spacecraft launch and ascent. The yoke and panels are interconnected by the hinges. The energy for the deployment is provided by the pre-loaded torsion springs located at each of the hinges. To synchronize the deployment motion of the panels, a synchronization system is mounted alongside each panel. The closed cable loop (CCL) is commonly used as a synchronous deploying control mechanism of the solar array [1–6]. The solar array deployment has been studied by many researchers.

***Author for Correspondence**
Yong-Gil Han
E-mail: YG.HAN@star-co.net.kp

Assistant Professor, Department of Mechanical Science and Technology, Kim Chaek University of Technology, Pyongyang, Democratic People's Republic of Korea

Receiving Date: June 30, 2025
Accepted Date: September 16, 2025
Published Date: September 25, 2025

Citation: Hyon-Mu Jo, Song-Hyok Kim, Ji-Hyon Kim, Ju-Song Thak, Yong-Gil Han. The Decision of the Maximum Synchronous Torque During the Solar Array Deployment Using the Closed Cable Loop. Journal of Aerospace Engineering & Technology. 2025; 15(3): 37–49p.

Narayana *et al*. took each deployment angle as the generalized coordinates and the synchronous torques at each joint as the generalized forces, and then, studied the solar array deployment by using ADAMS [7]. Li studied the synchronous torques and the change of the cable tension by using ADAMS and decided the pretension of the cable [8]. Here, the ratio of the change of the cable tension to the pretension was considered and the pretension was decided so that the change of the cable tension was not bigger than the pretension. Wang *et al*. explained the operation principle of a CCL and the cause of asynchronous phenomena [9]. He described the synchronous torque by a CCL as a function of the asynchronous angle and provided the better way to practice the synchronization of the solar array deployment. Chen provided a single-DOF analysis method for the deployment of the solar array, which considers that the solar array deployment using the CCLs is ideal and synchronous, and studied the deployment period and the angular velocity at the end of the deployment [10, 11]. It is simple and convenient to study the deployment period and angular velocity at the end of the deployment by using the single-DOF method. Chen also provided the method for calculation of the synchronous torque and analyzed the change of the cable tension and the asynchronous angle. Here, the equations of motion of each body (a yoke and three panels) were established, and the synchronous torques were calculated by using the angular velocity and the angular acceleration obtained from the single-DOF model. But the errors included in results of the synchronous torque were not analyzed and the calculation method of the maximum synchronous torque was not provided. Ding *et al*. provided the 4-DOF dynamic model of a solar array [2, 12]. The output torque of the root hinge drive assembly (RHDA) was calculated here, but the characteristics of the synchronous torque were not studied. The *n*-DOF dynamic model of a solar array, but this model is composed of matrices of high dimension ($(3+3n)\times(3+n)$), so it is complicated to analyze the solar array deployment using this model.

The synchronous torque directly affects to the deployment synchronization of a solar array and it is related with the structural parameters not only of the solar panels but also of the CCLs such as the stiffness coefficient, the pretension of the cable, and the diameter of pulleys. Furthermore, the maximum of the synchronous torque is the very important parameter because it is the base data for design of the CCLs to guarantee the successful deployment of the solar array. However, the characteristics of the synchronous torque were not studied in depth, especially, as there are no methods to decide the maximum of the synchronous torque. Multi-DOF dynamic models contain the asynchronous phenomena implicitly, so it is easier and convenient to consider the synchronous torque by using the multi-DOF dynamic model.

Multi-DOF models provided in previous studies have limitations in the application, because they were modeled under some conditions, for example, that all of the panels have the equal length. The panels of the solar array introduced by Haynie and Kriger were not same in length [13]. Its outer panel was longer than the inner panel. With the rapid development of astronautic technology, the growing requirements of the electrical power have the need to use large-area arrays and it makes the number of panels grow. Hence, it is needed to generalize the dynamic model to the case of more panels.

This study establishes a generalized multi-DOF deployment dynamic model of a solar array with *n* panels and proposes the calculation method of maximum of the synchronous torque based on the model.

DYNAMIC MODELING OF THE SOLAR ARRAY

Kinematics

The global position vector of an arbitrary point on the rigid body *i* can be expressed in terms of the translation and the rotation of the body, as shown in Figure 1 [6].

$$r^i = R^i + A^i \bar{u}^i \tag{1}$$

where, r^i is the global position vector of an arbitrary point P on the rigid body i, R^i the global position vector of the origin of the body coordinate system $X_1^i X_2^i X_3^i$, A^i rotation matrix that defines the

orientation of body *i* with respect to the global coordinate system $X_1X_2X_3$, $\bar{u}^i$ the position vector of an arbitrary point *P* in the body coordinate system $X_1^iX_2^iX_3^i$ which has a constant component.

A yoke and the solar panels are interconnected by the revolute hinges, so that the deployment motion can be considered as a planar motion [12]. Figure 2 shows the schematic representation of a solar array with the defined coordinate systems. It is clear that the orientation of all of the body coordinate systems can be coincided with the global coordinate system when the solar array is fully deployed.

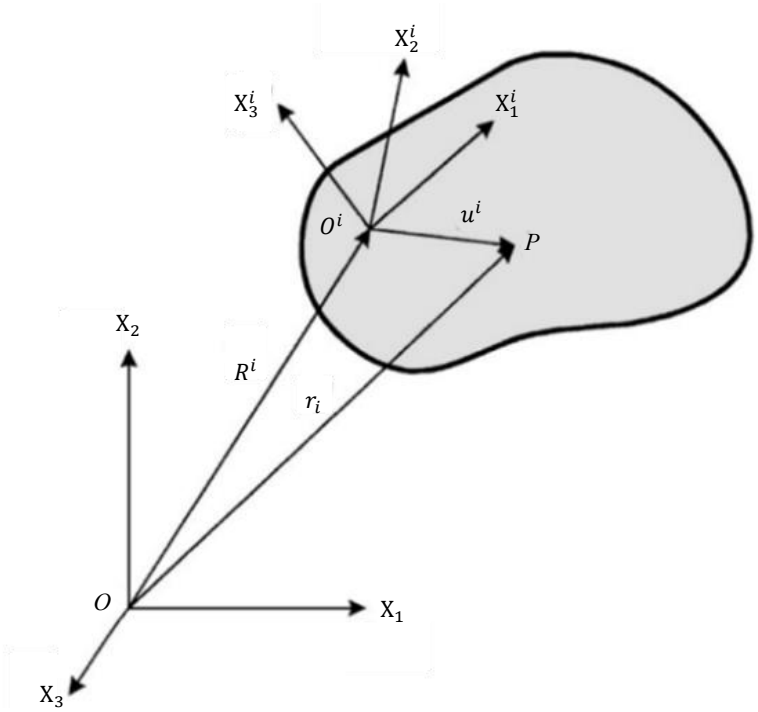

Figure 1. Global coordinate system and body coordinate system.

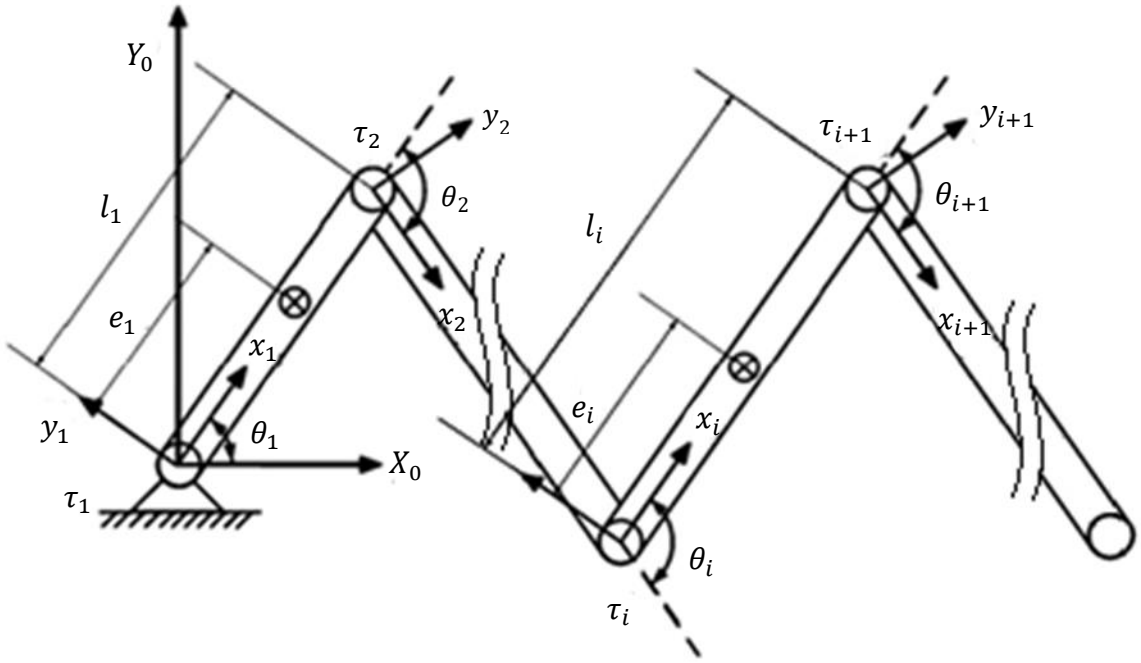

Figure 2. Coordinate systems of a solar array system.

The position vector of the mass center of each panel and the origin of the body coordinate systems can be described as follows:

$$r_c^i = R^i + A^i \bar{E}^i \tag{2}$$

$$R^i = R^{i-1} + A^{i-1}\bar{L}^{i-1} = \sum_{j=1}^{i-1} A^j \bar{L}^j \tag{3}$$

where, r_c^i represents the global position vector of the mass center of the *i*th panel, $\bar{E}^i$ and $\bar{L}^i$the local position vector of the mass center and length vector of the *i*th panel in the *i*th body coordinate system, respectively.

$$\bar{E}^i = [e_i \quad 0]^T \tag{4}$$

$$\bar{L}^i = [l_i \quad 0]^T \tag{5}$$

The rotation matrix from the *i*th body coordinate system to the global coordinate system is:

$$A^i = A^{i-1}A^{i,i-1} = \prod_{j=1}^{i} A^{j,j-1} \tag{6}$$

where, $A^{i,i-1}$ is the rotation matrix from the *i*th body coordinate system to the *i*-1th coordinate system.

$$A^{i,i-1} = \begin{bmatrix} cos\,\theta_i & -sin\,\theta_i \\ sin\,\theta_i & cos\,\theta_i \end{bmatrix} \tag{7}$$

Therefore, the rotation matrix, the position vector and the velocity vector of the mass center can be written as follows:

$$A^i = \begin{bmatrix} cos\,\alpha_i & -sin\,\alpha_i \\ sin\,\alpha_i & cos\,\alpha_i \end{bmatrix} \tag{8}$$

$$r_c^i = \left[\sum_{j=1}^{i} g_{ij}\, cos\,\alpha_j \quad \sum_{j=1}^{i} g_{ij}\, sin\,\alpha_i\right]^T \tag{9}$$

$$\dot{r}_c^i = \left[-\sum_{j=1}^{i} g_{ij}\dot{\alpha}_j\, sin\,\alpha_j \quad \sum_{j=1}^{i} g_{ij}\dot{\alpha}_j\, cos\,\alpha_j\right]^T \tag{10}$$

Where,

$$\alpha_i = \sum_{j=1}^{i} \theta_j,\ \dot{\alpha}_i = \sum_{j=1}^{i} \dot{\theta}_j \tag{11}$$

$$g_{ij} = \begin{cases} l_j, j \neq i \\ e_j, j = i \end{cases} \tag{12}$$

The angular velocity of the *i*th body coordinate system with respect to the global coordinate system can be described as follows:

$$\omega_i = \omega_{i-1} + \omega_{i,i-1} \tag{13}$$

where, ω_i is the angular velocity of the *i*th body coordinate system with respect to the global coordinate system and $\omega_{i,i-1}$ is one of the *i*th body coordinate systems with respect to the *i*-1th body coordinate system.

$$\omega_{i,i-1} = \dot{\theta}_i \tag{14}$$

Accordingly, Eq. (13) can be written as follows:

$$\omega_i = \sum_{j=1}^{i} \omega_{j,j-1} = \sum_{j=1}^{i} \dot{\theta}_j = \dot{\alpha}_i \tag{15}$$

Multi-DOF dynamic model

Let us derive the dynamic equation of the solar array with *n* panels (to be more exact, a yoke and *n*-1 panels). The degree of freedom is *n*. Let us take the deployment angle of each panel as the generalized coordinates as $q_i = \theta_i, i = 1, 2, \cdots, n$.

Then the kinetic energy of the *i*th panel is:

$$T^i = \frac{1}{2} m_i \dot{\boldsymbol{r}}_c^{i\,T} \dot{\boldsymbol{r}}_c^i + \frac{1}{2} J_c^i \omega_i^2 \tag{16}$$

where, m_i and J_c^i are the mass and the mass moment of inertia for the mass center of the *i*th panel, respectively.

The total kinetic energy of system can be obtained as follows:

$$T = \sum_{i=1}^{n} T^i = \frac{1}{2} \sum_{i=1}^{n} \left(J_c^i \dot{\alpha}_i^2 + m_i \sum_{j=1}^{i} g_{ij}^2 \dot{\alpha}_j^2 \right) + \sum_{i=2}^{n} \sum_{j=1}^{i-1} \sum_{k=j+1}^{i} m_i g_{ij} g_{ik} \dot{\alpha}_j \dot{\alpha}_k \cos\left(\alpha_j - \alpha_k\right) \tag{17}$$

The total potential energy of system can be expressed as follows:

$$U = \frac{1}{2} \sum_{i=1}^{n} k_i^s (\theta_{0i} - \theta_i)^2 \tag{18}$$

where, k_i^s and θ_{0i} are the stiffness coefficient and the preliminary displacement angle of torsion spring located at the *i*th joint, respectively.

Hence, the dynamic equation can be obtained as [14, 6]:

$$\frac{d}{dt}\left(\frac{\partial L}{\partial \dot{q}_i}\right) - \frac{\partial L}{\partial q_i} = Q_i, i = 1, 2, \cdots, n \tag{19}$$

where, $\dot{q}_i$ and Q_i are the generalized velocity and generalized force, respectively, and L is the Lagrangian.

$$L = T - U \tag{20}$$

The dynamic Eq. (19) can be written in the following matrix form:

$$M(\Theta)\ddot{\Theta} + V\left(\Theta, \dot{\Theta}\right) = \tau \tag{21}$$

where, $M(\Theta)$ is the mass matrix, $V\left(\Theta, \dot{\Theta}\right) = [V_1 \quad V_2 \quad \cdots \quad V_n]^T$ a vector of centrifugal and Coriolis terms, $\dot{\Theta} = [\dot{\theta}_1 \quad \dot{\theta}_2 \quad \cdots \quad \dot{\theta}_n]^T$ a vector of the joint angular velocity, $\ddot{\Theta} = [\ddot{\theta}_1 \quad \ddot{\theta}_2 \quad \cdots \quad \ddot{\theta}_n]^T$ a vector of the joint angular acceleration, $\tau = [\tau_1 \quad \tau_2 \quad \cdots \quad \tau_n]^T$ a vector of joint torque.

The mass matrix and the vector of centrifugal and Coriolis terms are as follows:

$$M(\Theta) = \begin{bmatrix} M_{11} & M_{12} & \cdots & M_{1n} \\ M_{21} & M_{22} & \cdots & M_{2n} \\ \vdots & \vdots & \ddots & \vdots \\ M_{n1} & M_{n2} & \cdots & M_{nn} \end{bmatrix}$$

$$M_{uv} = \sum_{i=1}^{n}\sum_{j=1}^{i} m_i g_{ij}^2 s_{uj} s_{vj} + \sum_{i=2}^{n} m_i \sum_{j=1}^{i-1}\sum_{k=j+1}^{i} g_{ij} g_{ik}\left(s_{uk} s_{vj} + s_{uj} s_{vk}\right) cos\left(\alpha_j - \alpha_k\right) + \sum_{i=1}^{n} J_c^i s_{ui} s_{vi}$$
$$u = 1,2,\cdots,n \qquad v = 1,2,\cdots,n \tag{22}$$

$$V_u = \sum_{i=2}^{n} m_i \sum_{j=1}^{i-1}\sum_{k=j+1}^{i} g_{ij} g_{ik}\left[\dot{\alpha}_j \dot{\alpha}_k \left(s_{uj} - s_{uk}\right) - \left(s_{uk}\dot{\alpha}_j + s_{uj}\dot{\alpha}_k\right)\left(\dot{\alpha}_j - \dot{\alpha}_k\right)\right] sin\left(\alpha_j - \alpha_k\right)$$
$$u = 1,2,\cdots,n \tag{23}$$

where,

$$s_{ij} = \begin{cases} 1, & j \geq i \\ 0, & j < i \end{cases} \tag{24}$$

$$\ddot{\alpha}_i = \sum_{j=1}^{i} \ddot{\theta}_j \tag{25}$$

The joint torque consists of the drive torques by the torsion springs and the synchronous torques by the CCLs.

$$\boldsymbol{\tau} = \boldsymbol{\tau}^S + \boldsymbol{\tau}^C \tag{26}$$

If there is a RHDA to control the deployment of the solar array, the drive torque of RHDA τ_A is also included in the root joint torque.

$$\tau_1 = \tau_1^S + \tau_1^C + \tau_A \tag{27}$$

The drive torque by torsion spring at the *i*th joint is:

$$\tau_i^S = k_i^S(\theta_{0i} - \theta_i) \tag{28}$$

The coefficients of Eq. (28) can be modified according to the ground test performance to compensate the joint resistance influence [2, 12].

And the synchronous torque by the CCLs at the *i*th joint is:

$$\tau_i^C = \tau_{i,i-1}^C + \tau_{i,i}^C$$
$$\tau_{i,j}^C = 2R_i \Delta F_j$$
$$\Delta F_i = \left(\frac{\theta_{i+1}(0)}{\theta_i(0)}\theta_i - \theta_{i+1}\right) R_{i+1} k_i^C \tag{29}$$

where, k_i^C and ΔF^i are the stiffness coefficient of the cable and the change of the cable tension of the *i*th CCL, R_i is the radius of the pulley located at the *i*th joint, $\tau_{i,j}^C$ the synchronous torque by the *j*th CCL at the *i*th joint.

This dynamic model can be applied for any solar array. For example, if a solar array has a yoke and three panels, of which the degree of freedom is 4, and the panels are same in length, that is, $l_2 = l_3 = l_4$, then the mass matrix and the vector of centrifugal and Coriolis terms coincide with the result provided by Ding and Li [2].

CALCULATION OF THE MAXIMUM SYNCHRONOUS TORQUE

The synchronization of the solar array deployment is closely related to the structural parameters of the CCLs.

During the deployment of the solar array, the cable tension is changed according to the deployment angle and the synchronous torque by a CCL is proportional to the change of the cable tension. And the change of the cable tension is proportional to the stiffness coefficient and the asynchronous angle.

If the pretension of the cable of the CCLs is too low, the cable becomes loose, and it affects to the synchronization of the solar array deployment. Contrarily, if the pretension is too high, the frictional resistance torque gets higher, and the stress of the cable can even reach to the limit of strength or the cable may break down by the additional tension. So, the pretension of the cable of the CCLs should be as low as possible with guaranteeing the synchronization of the deployment, and also, it should not be lower than the change of the tension.

Like these, the synchronous torque is not only related with the characteristics of the solar array deployment using the CCLs, but also significant data for the design of the CCLs. Hence, the calculation method of the synchronous torque is provided in this section.

Calculation of the Synchronous Torque

Let us derive the formula to calculate the synchronous torque for the ideal synchronization of the solar array deployment. The condition for the ideal synchronization is:

$$\frac{\theta_{i+1}(0)}{\theta_i(0)}\theta_i - \theta_{i+1} = 0, i = 1, 2, \cdots, n-1 \tag{30}$$

Hence, we can obtain the following equations:

$$\begin{cases} \theta_i = c_i\theta_1 \\ \dot{\theta}_i = c_i\dot{\theta}_1, i = 1, 2, \cdots, n \\ \ddot{\theta}_i = c_i\ddot{\theta}_1 \end{cases} \tag{31}$$

where,

$$c_i = \frac{\theta_i(0)}{\theta_1(0)} \tag{32}$$

The total kinetic energy of system can be described by θ_1 and $\dot{\theta}_1$ as follows:

$$T = \sum_{i=1}^{n} T^i = \frac{1}{2}J(\theta_1)\dot{\theta}_1^2 \tag{33}$$

where, J is the corresponding mass moment of inertia of system.

$$J = \sum_{i=1}^{n}\left(J_c^i d_i^2 + \sum_{j=1}^{i} m_i g_{ij}^2 d_j^2\right) + 2\sum_{i=2}^{n}\sum_{j=1}^{i-1}\sum_{k=j+1}^{i} m_i g_{ij} g_{ik} d_j d_k \cos\left(d_j - d_k\right)\theta_1 \tag{34}$$

$$d_i = \frac{\alpha_i(0)}{\theta_1(0)} = \sum_{j=1}^{i} c_j \tag{35}$$

And its derivative can be obtained as follows:

$$J' = -2\sum_{i=2}^{n}\sum_{j=1}^{i-1}\sum_{k=j+1}^{i} m_i g_{ij} g_{ik} d_j d_k\left(d_j - d_k\right)\sin\left(d_j - d_k\right)\theta_1 \tag{36}$$

The total potential energy of system and its derivative can be expressed as follows:

$$U = \frac{1}{2}\sum_{i=1}^{n} k_i^s(\theta_{0i} - c_i\theta_1)^2 \tag{37}$$

$$U' = -\sum_{i=1}^{n} k_i^s c_i(\theta_{0i} - c_i\theta_1) \tag{38}$$

Considering the initial condition, we can write the following equation from the energy conservation law:

$$T + U = U_0 \tag{39}$$

where, U_0 represents the initial potential energy.

The angular velocity and the angular acceleration can be obtained from Eqs. (33) and (39).

$$\dot{\theta}_1(\theta_1) = -\sqrt{\frac{2(U_0 - U)}{J}} \tag{40}$$

$$\ddot{\theta}_1(\theta_1) = -\frac{J'}{J^2}(U_0 - U) - \frac{U'}{J} \tag{41}$$

where, the sign of the angular velocity "-" is because the deployment of the yoke starts at 90°and ends at 0°. Eqs. (40) and (41) indicate that the angular velocity and angular acceleration of the deployment are represented by deployment angle of the yoke, when the solar array deployment is ideally synchronous.

From Eqs. (21) and (26), the synchronous torque can be expressed as follows:

$$\tau^c = M(\Theta)\ddot{\Theta} + V\left(\Theta, \dot{\Theta}\right) - \tau^s \tag{42}$$

Considering Eqs. (40) and (41), the synchronous torque depends on deployment angle of the yoke θ_1.

$$\tau^c(\theta_1) = M(\theta_1)\ddot{\theta}_1(\theta_1) + V(\theta_1) - \tau^s(\theta_1) \tag{43}$$

And also, we can write the relation between the synchronous torques at both the joints by a CCL.

$$\tau_{i,i}^c = -\frac{c_{i+1}}{c_i}\tau_{i+1,i}^c \tag{44}$$

Considering Eqs. (29) and (44), we can represent the synchronous torque at the *i*th joint by the *i*th CCL by deployment angle from Eq. (43).

$$\tau_{i,i}^c(\theta_1) = \sum_{j=1}^{n} c_j M_{ij}(\theta_1)\,\ddot{\theta}_1(\theta_1) + V_i(\theta_1) - \tau_i^s(\theta_1) + \frac{c_{i-1}}{c_i}\tau_{i-1,i-1}^c(\theta_1),\ i = 1,2,\cdots,n-1 \tag{45}$$

Characteristics of the synchronous torque

The characteristics of the synchronous torque is analyzed by using the above calculation method. Tables 1 and 2 show the structural parameters of the yoke and the solar panels, and the torsion springs, respectively.

Table 1. Structural parameters of the yoke and solar panels.

Parameter	Yoke	Solar panel
Mass (kg)	1.46	11.95
Mass moment of inertia for the mass center (kgm^2)	0.05	1.45
Length (m)	0.66	1.26
Position of the mass center (m)	0.42	0.63

Table 2. Parameters of torsion springs.

Parameter	Root hinge	Panel-panel hinge	
		Odd index	*Even index*
Stiffness coefficient (Nmm/°)	2.7	1.35	1.35
Preload torque (Nm)	–0.081	–0.081	0.081
Initial displacement (°)	90	–180	180

Table 3 Characteristics of the synchronous torque.

Number of panels (including yoke)	CCLs	Maximum of the synchronous torque	
		Value (Nm)	*Deployment angle (°)*
n=2	CCL-1	0.83	12.0
n=3	CCL-1	–2.46	8.4
	CCL-2	–1.50	8.1
n=4	CCL-1	–3.13	6.6
	CCL-2	–1.40	6.9
	CCL-3	1.40	6.6
n=5	CCL-1	–11.66	5.6
	CCL-2	–4.92	5.9
	CCL-3	–0.84	5.5
	CCL-4	–2.94	5.7
n=6	CCL-1	–17.05	5.0
	CCL-2	–6.53	5.1
	CCL-3	–0.97	4.6
	CCL-4	–3.23	5.1
	CCL-5	2.43	5.0

Figure 3 shows the curve of the synchronous torques by the CCLs with deployment angle in the case of four panels. During the deployment, the angle of the yoke θ_1 decreases from 90 to 0°. The process of the deployment can be divided into two intervals according to the rate of change of the synchronous torque. In the first interval (right side of each graph), the synchronous torque changes slowly, while in the second interval (left side of each graph), it changes rapidly. What is more important is that the synchronous torque reaches to the absolute maximum in the second interval.

Table 3 gives the characteristics of the synchronous torque of the solar arrays with different number of panels. As we can see from the table, the maximum of the synchronous torque of the CCL-1 is the biggest of all. In addition to this, with the bigger number of panels, the synchronous torque reaches to the bigger maximum at the less deployment angle.

Approximate Calculation of the Maximum Synchronous Torque

The synchronous torque, of course, can be calculated by the deployment angle using Eq. (45). But it is difficult to calculate the maximum of the synchronous torque directly from it. So, a method to calculate the maximum of the synchronous torque is given. Let us use the polynomial approximation and its differentiation.

As mentioned above, the synchronous torque reaches to the maximum in the second interval. So, Eq. (45) can be approximated in the second interval as a cubic polynomial as follows:

$$\tau_{i,i}^{c}(\theta_1) = a_1^i \theta_1^3 + a_2^i \theta_1^2 + a_3^i \theta_1 + a_4^i \tag{46}$$

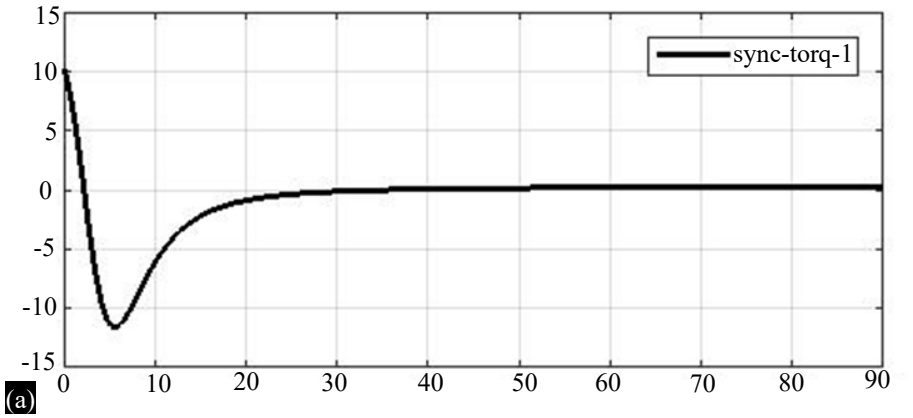

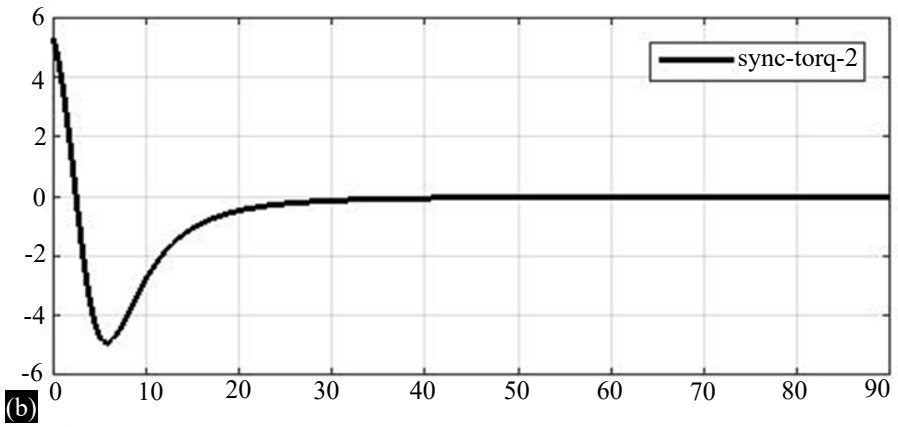

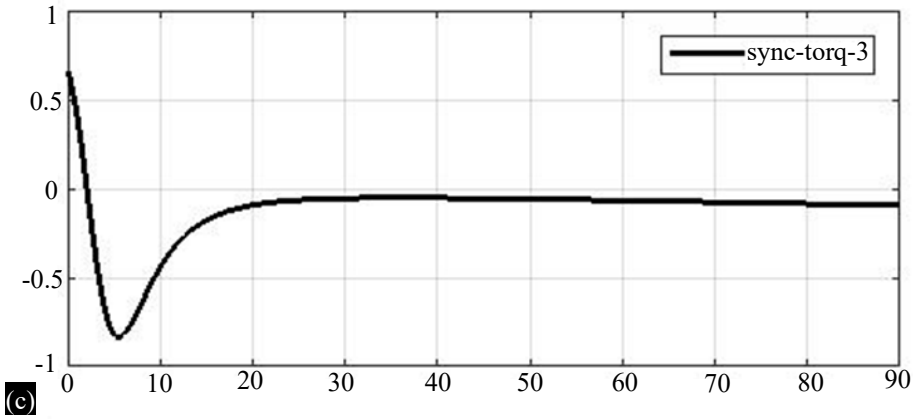

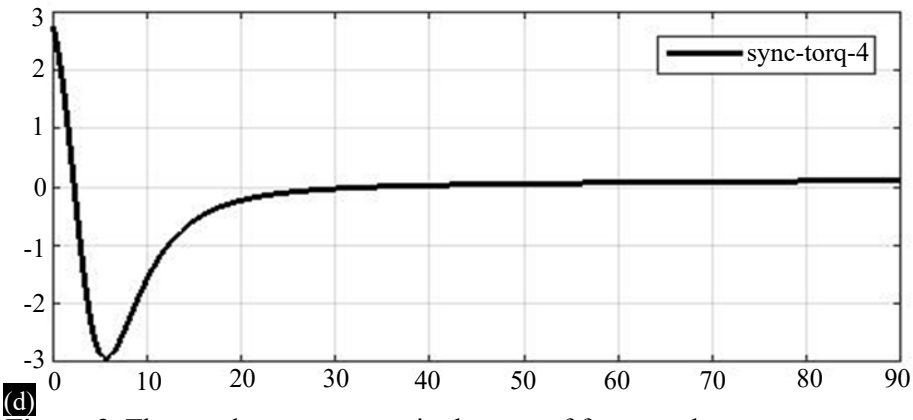

Figure 3. The synchronous torque in the case of four panels:
(a) CCL-1, (b) CCL-2, (c) CCL-3, and (d) CCL-4.

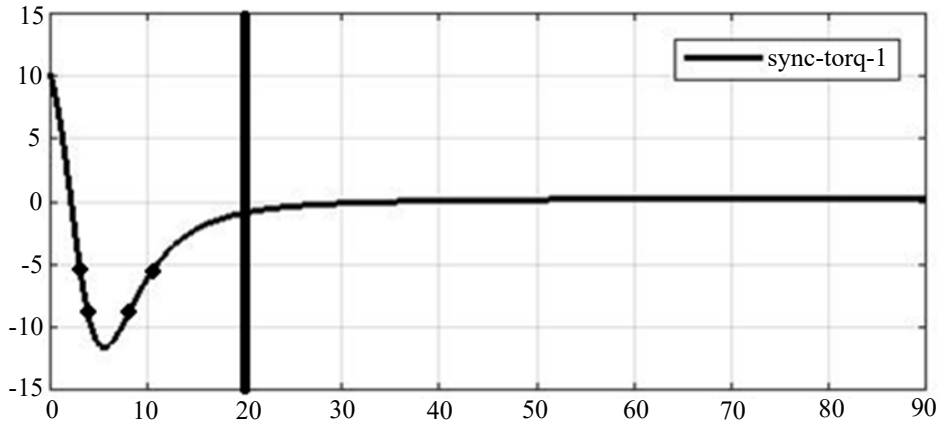

Figure 4. Sample points.

The coefficients of the polynomials can be obtained by catching four or more adequate sample points (Figure 4).

Then, the extremal point can be obtained as follows:

$$\theta_{1,ext}^{i} = \frac{-2a_2^i \pm \sqrt{\left(2a_2^i\right)^2 - 12a_1^i a_3^i}}{6a_3^i} \tag{47}$$

There are two roots and the root satisfying the following condition is the extremal point of maximum torque.

$$\text{sign}\left(\tau_{i,i}^{c}(\theta_{12}) - \tau_{i,i}^{c}(\theta_{11})\right)\left(6a_3^i\theta_{1,ext}^{i} + 2a_2^i\right) < 0 \tag{48}$$

where, sign(*) is the sign function.

Substituting Eq. (47) into Eq. (46), we can the maximum synchronous torque as follows:

$$\tau_{i,i,ext}^{c} = \tau_{i,i}^{c}\left(\theta_{1,ext}^{i}\right) = a_3^i\left(\theta_{1,ext}^{i}\right)^3 + a_2^i\left(\theta_{1,ext}^{i}\right)^2 + a_1^i\theta_{1,ext}^{i} + a_0^i \tag{49}$$

Eq. (49) gives the approximate value of absolute maximum of the synchronous torque by the *i*th CCL. From the maximum, the diameters of pulleys and the changes of the cable tensions of the CCLs can be obtained, and the pretension of the cable can be decided. And also, the stiffness coefficient of the cable can be decided according to the given asynchronous angle.

NUMERICAL RESULTS

The accuracy of the calculation method of the maximum synchronous torque is verified.

First, the maximum of the synchronous torque of the solar array with the different number of panels is calculated from Eq. (49). Then, the stiffness coefficient of the cable is decided according to the given asynchronous angle while the diameter of pulleys of root hinge and panel-panel hinge are 100 and 50 mm, respectively. In general, the CCLs of a solar array employ the same cable, so the stiffness coefficients take one of CCL-1 by which the maximum synchronous torque is the biggest. The stiffness coefficient can be calculated from the maximum of the synchronous torque as follows:

$$k_1^c = \frac{\tau_{1,1,ext}^{c}}{2R_1R_2\Delta\theta_1} \tag{50}$$

Table 4 The maximum synchronous torque with the asynchronous angle (Nm).

Asynchronous angle (°)	Number of panels			
	3	*4*	*5*	*6*
0.0	2.461	3.128	11.600	17.050
0.5	2.449	3.113	11.562	17.010
2.0	2.434	3.097	11.526	16.962
1.5	2.418	3.078	11.484	16.905
2.0	2.399	3.057	11.413	16.812
2.5	2.350	3.003	11.227	16.600
3.0	2.224	2.853	10.840	16.100

Table 5 Relative error of the maximum synchronous torque with the asynchronous angle (%).

Asynchronous angle (°)	Number of panels			
	3	*4*	*5*	*6*
0.5	0.5	0.5	0.3	0.2
2.0	1.1	1.0	0.6	0.5
1.5	1.7	1.6	1.0	0.9
2.0	2.5	2.3	1.6	1.4
2.5	4.5	4.0	3.2	2.6
3.0	9.6	8.8	6.6	5.6

where, $\Delta\theta_1$ is the asynchronous angle between the two joints wrapped by CCL-1.

Then, this stiffness coefficient is substituted into the multi-DOF dynamic model (Eq. (21)) and the maximum of the real synchronous torque can be obtained by solving the equation.

Table 4 shows the maximum synchronous torque by CCL-1 according to the asynchronous angle with different number of panels. The values in the first row is corresponding to the ideal synchronization, that is, the asynchronous angle is 0° and it is obtained by the calculation method of maximum synchronous torque (Eq. (49)). And Table 5 shows its relative error.

The result indicates that the bigger the asynchronous angle gets, the bigger the relative error is. This means that the calculation method is more accurate when the cable is more stiff. And when the number of panels is increasing, the relative error gets smaller for the same asynchronous angle. This can be explained by the fact that the maximum of the synchronous torque gets bigger as the number of panels is increasing. The relative error is smaller than 5% when the asynchronous angle is not bigger than 2.5°. This indicates that the calculation method of maximum synchronous torque has enough accuracy when the asynchronous angle is not bigger than 2.5°. In other words, this method can be used only when the cable is stiff sufficiently, so that the asynchronous angle is not bigger than 2.5°.

CONCLUSION

The study on the solar array deployment has the great significance for the successful operation of a spacecraft in space. This study provides the generalized multi-DOF dynamic model of the solar array with *n* panels. The dynamic model can be applied to any solar array, and the characteristics of the deployment such as the deployment period, angular velocity, the synchronous torque can be obtained by the model. This model can also be used to obtain the output torque of RHDA. The calculation formula of the synchronous torque for the ideal synchronization is derived and its characteristics are analyzed. Then the calculation method of the maximum synchronous torque is provided and its accuracy is verified. The results indicate that the method has enough accuracy when the asynchronous angle is not

bigger than 2.5°. From the maximum synchronous torque, the design parameters of the CCLs, such as the diameter of pulleys, the stiffness coefficient and the pretension of the cable, can be decided.

REFERENCES

1. Birhanu F, Chen ZB, Ma WS. Modeling and simulation of satellite solar panel deployment and locking. Inf Technol J. 2010; 9(3): 600–4.
2. Ding XL, Li X. Design and test analysis of a solar array root hinge drive assembly. Chin J Mech Eng. 2014; 27(5): 909–18.
3. Jorgensen JR, Louis EL, Hinkle JD, Silver MJ. Dynamics of an elastically deployable solar array: ground test model validation. In: AIAA Paper 2005-1942. 2005.
4. Li HQ, Liu XF, Duan LC, Cai GP. Deployment and control of spacecraft solar array considering joint stick-slip friction. Aerosp Sci Technol. 2015; 42: 342–52.
5. Li XZ, Zheng FB, Yang Z, Xi BC. Dynamic response of solar panel deployment on spacecraft system considering joint clearance. Acta Astronaut. 2012; 81: 174–85.
6. Wallrapp O, Wiedemann S. Simulation of the deployment of a flexible solar array. Multibody Syst Dyn. 2002; 7(1): 101–25.
7. Narayana BL, Nagaraj BP, Nataraju BS. Deployment dynamics of the solar array with body rates. In: International ADAMS User Conference. 2000.
8. Li WT. The design and analysis of close cable loop of the solar array. Chin Space Sci Technol. 2006; 26(2): 52–7. Chinese.
9. Wang TH, Kong XR, Wang BL, Ma XR. The research on principle and function of closed-loop configuration of solar arrays. J Astronautics. 2000;21(3):29–33.
10. Chen LM. Analysis of the secondary deployment motion of the solar array. Spacecraft Eng. 2001; 10(3): 19–23. Chinese.
11. Chen LM. Analysis of the change of the closed cable loop tension of the solar array. Spacecraft Eng. 1999; 8(4): 9–13. Chinese.
12. Ding XL, Li X, Xu K, Yang QL, Pu HL. Study on the behavior of the solar array deployment with root hinge drive assembly. Chin J Aeronaut. 2012; 25: 276–84.
13. Haynie T, Kriger A. Mechanisms for restraining and deploying a 50-kW solar array. In: 3rd Aerospace Mechanisms Symposium. 1969.
14. Shabana AA. Dynamics of multibody systems. 4th Edn. Cambridge: Cambridge University Press; 2013.

